

Detection and characterization of breast masses with ultrasound tomography: Clinical results

Neb Duric, Peter Littrup, Cuiping Li, Olsi Rama,
Lisa Bey-Knight, Steven Schmidt and Jessica Lupinacci.

Karmanos Cancer Institute, Wayne State University, 4100 John R. Street, Detroit, MI 48201

ABSTRACT

We report on a continuing assessment of the in-vivo performance of an operator independent breast imaging device based on the principles of acoustic tomography. This study highlights the feasibility of mass characterization using criteria derived from reflection, sound speed and attenuation imaging. The data were collected with a clinical prototype at the Karmanos Cancer Institute in Detroit MI from patients recruited at our breast center. Tomographic sets of images were constructed from the data and used to form 3-D image stacks corresponding to the volume of the breast. Masses were identified independently by either ultrasound or biopsy and their locations determined from conventional mammography and ultrasound exams. The nature of the mass and its location were used to assess the feasibility of our prototype to detect and characterize masses in a case-following scenario.

Our techniques generated whole breast reflection images as well as images of the acoustic parameters of sound speed and attenuation. The combination of these images reveals major breast anatomy, including fat, parenchyma, fibrous stroma and masses. The three types of images are intrinsically co-registered because the reconstructions are performed using a common data set acquired by the prototype. Fusion imaging, utilizing thresholding, is shown to visualize mass characterization and facilitates separation of cancer from benign masses. These initial results indicate that operator-independent whole-breast imaging and the detection and a characterization of cancerous breast masses are feasible using acoustic tomography techniques.

Keywords: Breast imaging, breast masses, image fusion, ultrasound tomography

1. INTRODUCTION

Mammography screening has been shown to reduce the mortality rate in multiple screening trials¹. However, diagnostic mammography generates many abnormal findings not related to cancer that leads to additional, costly imaging procedures and biopsies². *Specificity* is the most important benefit-cost factor impacting early detection testing³⁻⁵. A mammogram finding is not specific because its two main diagnostic criteria, the identification, of calcium deposits and masses, are also seen with non-cancerous breast changes. The differentiation of benign from malignant tissue by mammography is further hampered by the added density of normal breast parenchyma.

DCE-MRI is making increasing inroads into diagnostic breast imaging by virtue of its high sensitivity and operator independence⁶⁻⁷. Consequently, MRI is now viewed as the gold-standard for breast cancer early detection and screening of high risk women, particularly for those with dense breasts⁸⁻⁹. However, the exams are both long and costly and the equipment and room preparation costs are extremely high, thereby limiting access for many women. For these reasons, mammography is most commonly complemented with ultrasound which helps differentiate cysts from solid masses and has become the dominant mode for guiding needle biopsy. Recent studies have demonstrated the effectiveness of ultrasound imaging in detecting breast cancer¹⁰⁻¹², particularly for women with dense breasts. As a result of these studies, ultrasound is increasingly being examined for its potential as a screening tool. The ongoing ACRIN 6666 study, funded by the Avon Foundation and the NCI, represents a definitive trial evaluating the potential of ultrasound as a screening tool¹¹. The latest reports have shown the potential to screen for small breast masses otherwise missed by mammography¹². Despite these successes, US is unlikely to gain broad community acceptance for the following reasons:

(i) The added cancers found by US are offset by an increased burden of false positives¹², indicating that characterization of small masses by conventional US is limited. (ii) The operator dependent nature of ultrasound will prevent uniform replication of results. (iii) The associated small-aperture-imaging leads to long exam times and the need to “stitch” the localized images into a whole breast view. The gap between promise and practical implementation of screening US, therefore, still appears so wide that expensive modalities other than MRI have been considered. Breast Specific Gamma Imaging (BSGI) has had much less clinical testing than MRI but proponents have suggested that despite its similar requirement of an injected contrast agent, it could be much less expensive than MRI¹³. However, the resolution and planar projections of BSGI limit detailed anatomic comparisons to MRI, let alone identification or characterization of any masses other than the cancer which generated the suspicion on palpation or mammogram. The cost, access and ease-of-use of any diagnostic modality will determine its broad acceptance for screening. Addressing the problems of current US to give it the volumetric image acquisition and operator independence of MRI would be a major advance toward a clinically successful screening option.

In 1976, Greenleaf et al¹⁴ made the seminal observation that acoustic measurements made with transmission ultrasound could be used to characterize breast tissue. On the basis of these studies, they concluded that using the imaging parameters of sound speed and attenuation (henceforth the *Greenleaf* criteria) could help differentiate benign masses from cancer. Using a number of in-vitro samples of various types of breast tissue, they were able to quantify the acoustic sound speed (propagation velocity of an ultrasound pulse passing through the tissue) and attenuation (the reduction in pulse amplitude as it propagates through the tissue). They then demonstrated that in a plot of sound-speed versus attenuation, the benign and malignant masses were well separated. As a direct result of this and other similar studies, a number of investigators developed operator-independent ultrasound scanners in an attempt to measure the *Greenleaf* criteria with in-vivo scans.¹⁵⁻²¹ Examples include the work of Carson et al (U. Michigan)¹⁵, Andre et al (UCSD)¹⁶, Johnson et al¹⁷ (TechniScan Medical Systems), Marmarelis et al (USC)¹⁸, Liu and Waag (U. Rochester)¹⁹ and Duric and Littrup et al²⁰⁻²¹ (KCI).

In an ongoing study at the Karmanos Cancer Institute, we are investigating the performance of an operator independent whole-breast ultrasound imaging system in a clinical setting. The purpose of this paper is to describe the study and to present and discuss *in vivo* breast imaging results.

2. METHODS

2.1. The ultrasound tomography (UST) concept

The essential scientific idea behind UST is that *the interaction of sound waves with tissue yields a signatures that can be imaged tomographically*. The fundamental physical basis of the concept can be understood with the aid of Figure 1.

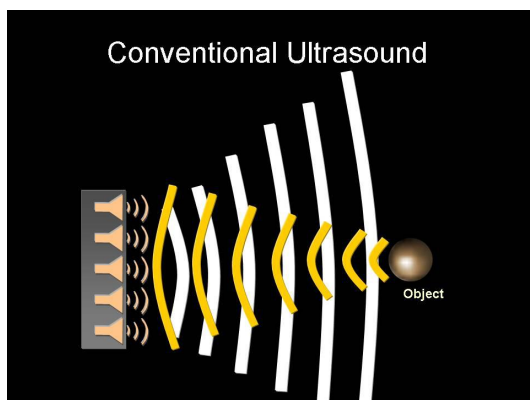


Figure 1(a): In conventional ultrasound, a pulse is emitted toward a target (white wave fronts) and the subsequent reflections off the target (yellow wave fronts) are recorded by the ultrasound detector. Only those reflections that travel directly back to the source are recorded.

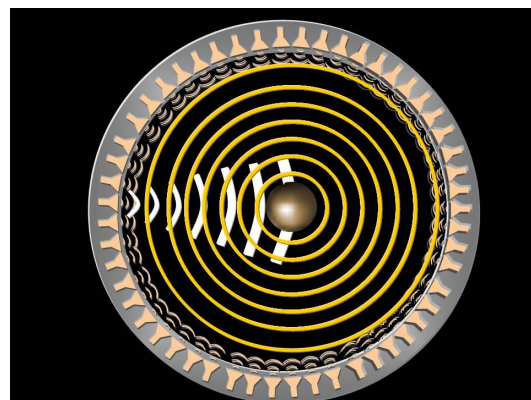


Figure 1(b): In reality, when ultrasound pulses are directed into human tissue they scatter off the tissue in all possible directions (yellow wave fronts). By surrounding the target with sensors, all of the scattered wave fronts can be recorded. Consequently, much more information about the tissue can be extracted.

Conventional ultrasound records only a small fraction of the scattered field and, therefore, a small fraction of the information about the tissue being examined. On the other hand, in the UST concept, most of the scattered field is detected. The additional information, ignored by conventional ultrasound methods, has the potential to yield a more accurate and complete assessment of the tissue characteristics. Furthermore, unlike mammography, UST produces a 3-D image that renders the entire volume of the breast, much like MRI. Reconstruction algorithms operating on the recorded data allow visualizations of the tissue parameters. The resulting images contain additional quantitative information that can be used to help extract the cancer signatures.

2.2. The UST Prototype

We have constructed a clinical prototype (Figure 2) to test the above concept in a clinical environment. The prototype has been housed at the Karmanos Cancer Institute, in a dedicated exam room, measuring 10 x 15 feet, in the Alexander J. Walt Comprehensive Breast Center. The device was installed in August 2004 and was thoroughly tested with simple and complex phantoms and subsequently used to scan patients. A typical whole breast exam takes about 1 minute to perform.

The total time the patient spends in the exam room is about 5 minutes. A patient exam begins with the patient lying prone on the UST table. The table consists of flexible sailcloth, which contours to the patient's body, thereby increasing access to the axilla regions of the breast and increasing patient comfort. The breast is suspended in the imaging tank that lies below the table, through a hole in the table. The imaging tank is filled with warm, clean water. The ultrasound sensor, in the shape of a ring, surrounds the breast and moves from the chest wall to the nipple region of the breast on a motorized gantry, gathering data along the way (as shown in Figure 3).

The images are reconstructed from the data acquired in this manner. Typically, reflection, sound speed and attenuation images are generated for each position of the transducer, yielding a stack (around 75 slices) of each type of image. The images are constructed from the same raw data set and are therefore registered on the same absolute grid, facilitating image fusion. Reflection images are reconstructed using algorithms that incorporate the concepts of aperture synthesis and migration and are based on those described in previous publications²¹. The sound speed and attenuation images are produced from algorithms that utilize "bent-ray" tomographic techniques. The latter techniques use ray-approximations for greater computational efficiency while accounting for refractive effects²⁶⁻²⁸.

Patients were recruited on the basis of having suspicious masses on mammography and are subsequently examined with the prototype. All imaging procedures are performed under an Institutional Review Board (IRB) approved protocol and in compliance with the Health Insurance Portability and Accountability Act (HIPAA).

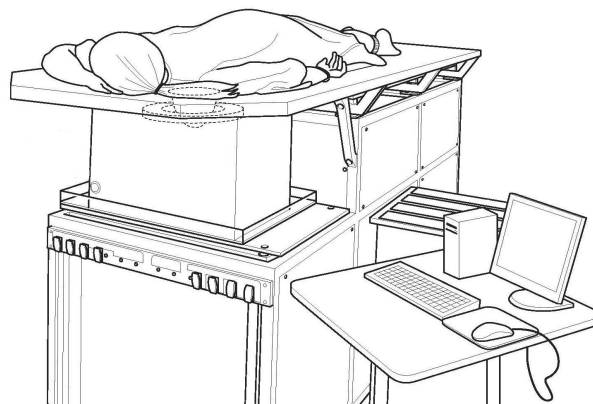


Figure 2: The clinical prototype. A patient lies in the prone position such that the breast is suspended inside a water tank that contains the ultrasound sensor. The water acts as a coupling medium to ensure that the acoustic waves can penetrate the breast efficiently.

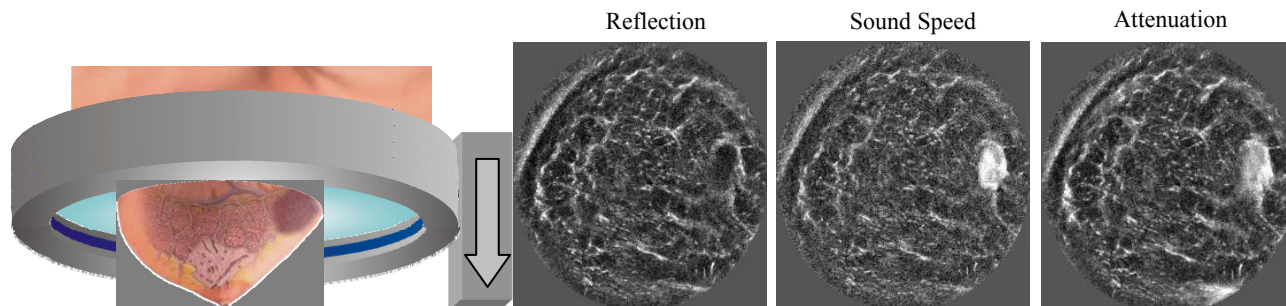


Figure 3: The ultrasound ring array (grey) surrounds the breast as it moves on a vertical trajectory from the chest wall to the nipple. At discrete steps along the way it acquires data at up to 75 positions. Each such dataset yields images of reflectivity, sound speed and attenuation, as shown on the right. The images show an irregular hypoechoic mass, at 2:00, that has high sound speed and attenuation. Since the images are constructed from the same data, they are intrinsically registered, allowing fast and accurate image fusion.

3. RESULTS AND DISCUSSION

3.1. Breast Anatomy

Images of all patients were constructed from the UST data and compared to standard imaging and biopsy. The initial focus of the study was to determine how reliably and accurately the breast architecture could be measured. Figure 4 illustrates a comparison of anatomy visualized with UST compared to that of MRI for the same patient. The MRI image (right image, fat subtracted, T1-weighted) shows the presence of fatty tissue (dark grey), parenchyma (light grey) and fibrous stroma (light bands). The corresponding UST image shows fatty tissue (dark) parenchyma (light grey) and fibrous stroma (white bands). It appears that our UST technique images the same anatomical components.

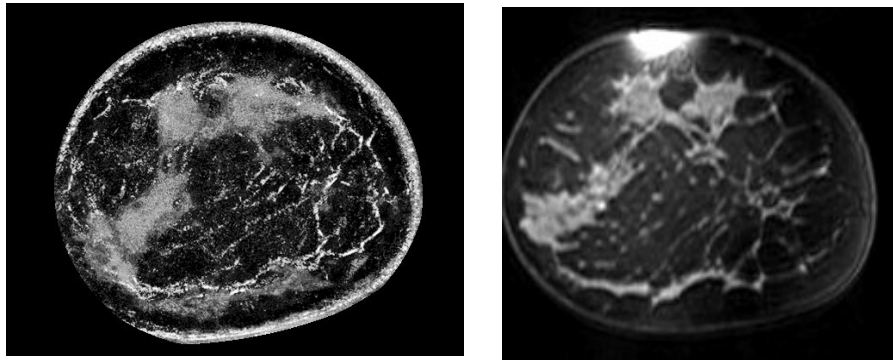


Figure 4 (Left) UST fusion image using reflection, sound speed and attenuation data shows comparable anatomic distribution of fat, fibroglandular tissue and fibrous bands as the MRI image **(Right)** from a corresponding coronal level through the breast.

3.2. Detection and characterization of breast masses

Analyses of the UST images suggests that mass attributes noted by current US-BIRADS criteria, such as mass shape, acoustic mass properties and architecture of the tumor environment, can be measured. Additionally, the measurable parameters of sound speed and attenuation are unique to transmission ultrasound, as first defined by Greenleaf¹⁴. They represent the internal acoustic properties of the mass that can be measured quantitatively in the UST sound speed and attenuation images.

Figure 3 shows cross-sectional UST images from an exam of a patient diagnosed with a 25 mm cancerous mass. The reflection image on the left shows a hypo-echoic region with thick, irregular margins, consistent with *US BIRADS* characterizations of cancer. Added diagnostic criteria are demonstrated in the remaining images. The middle image was constructed by superimposing a sound speed image on the reflection image, thresholded at a value of 1500 m/sec. The mass clearly displays an elevated sound speed relative to a background that is almost entirely below the threshold. In the rightmost panel, an attenuation image, thresholded at a value of 0.20 dB/cm, is shown superimposed on the reflection image. A local enhancement in attenuation is evident.

The ability to image multiple tissue parameters has led us to investigate the use of reflection, sound speed and attenuation parameters to characterize breast masses. The methodology we are pursuing can be visualized with the following illustrative examples.

Multi-parameter images of a cyst. Figure 5 shows reconstructions of reflection, sound speed and attenuation images for a cross-section of a breast containing a cyst.

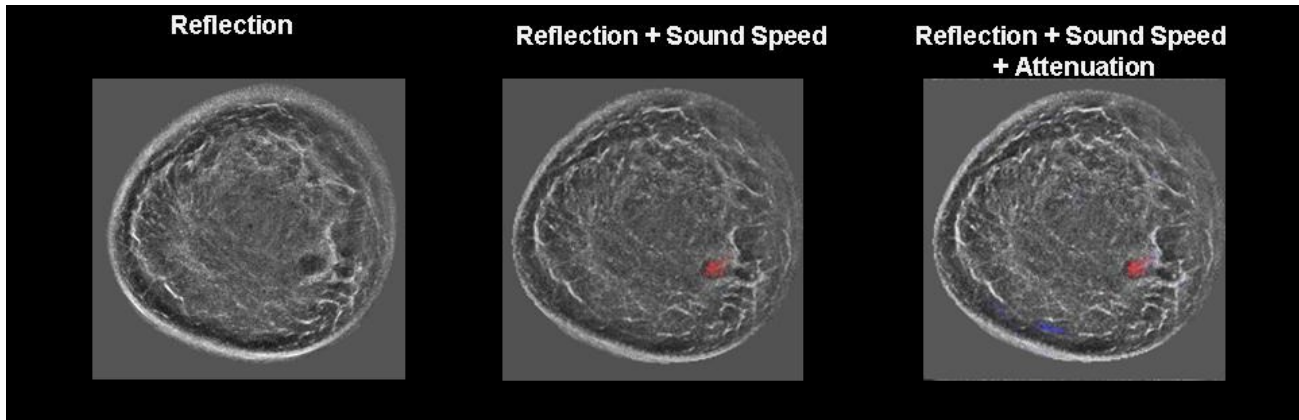


Figure 5. From left to right, reflection, sound speed and attenuation images of a 10 mm sized cyst in approximately the 4 o'clock, mid position of the breast. The thresholded sound speed image is rendered in red while the thresholded attenuation image is blue.

The cyst appears as a round, anechoic region on the reflection images, similar to its appearance on standard ultrasound images. The sound speed image shows a slight local elevation in sound speed. However, no distinct elevated attenuation region is evident relative to background tissue. The latter is to be expected because cysts should have minimal attenuation owing to their largely liquid nature. The elevated sound speed is the result of the fact that water at body temperature (sound speed of ~ 1.5 km/s) has a higher sound speed than fat.

Multi-parameter images of a Fibroadenoma. Figure 6 illustrates the properties of a fibroadenoma. Shown are reflection, sound speed and attenuation images of a 1cm fibroadenoma at approximately the 2 o'clock position.

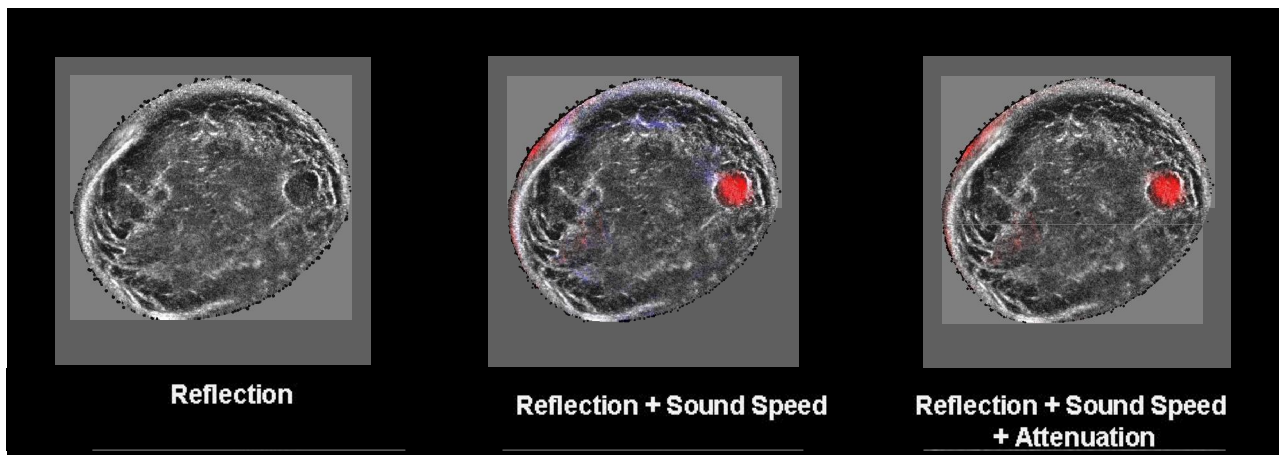


Figure 6: From left to right, reflection, sound speed and attenuation images of a fibroadenoma in approximately the 2 o'clock, far position of the breast.

The fibroadenoma appears as an oval, slightly hypoechoic region on the reflection images, similar to its appearance on standard ultrasound images. The sound speed image shows a strong local elevation in sound speed. However, no distinct elevated attenuation region is evident relative to background tissue.

Multi-parameter images of a cancer. Figure 7 shows analogous images for a cancer. The 2.5 cm mass, located in approximately the 10 o'clock near position, demonstrates a nearly isoechoic texture in reflection, and elevated sound speed and attenuation. Unlike the benign cysts noted above, the characteristics of the cancer deviate from those of the benign masses. The most obvious difference is the elevated attenuation relative to background tissue.

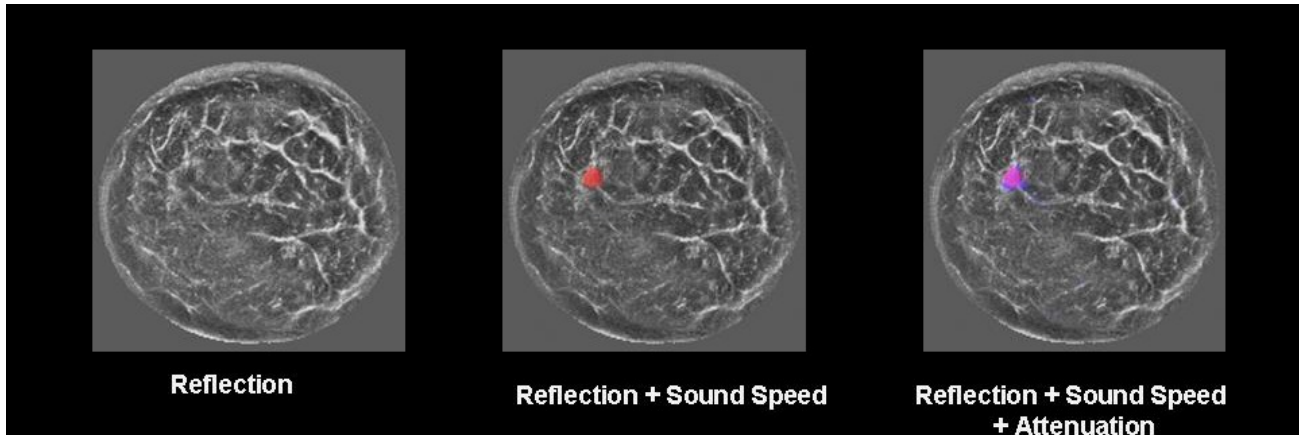


Figure 7. From left to right, reflection, sounds speed and attenuation images of a 2.5 cm sized cancer in approximately the 10 o'clock, mid position of the breast.

Statistical Analysis: We have performed an analysis to quantify the apparent differences in mass properties. We measured the mean attenuation and sound speed for 36 masses, relative to the surrounding tissue. Measurements were performed on the slice in which the mass was the most prominent. The reflection images were used to determine the boundaries of the mass and therefore the area over which the average values were calculated. The resulting values of the sound speed and attenuation were then plotted on a scatter plot, as shown in Figure 9.

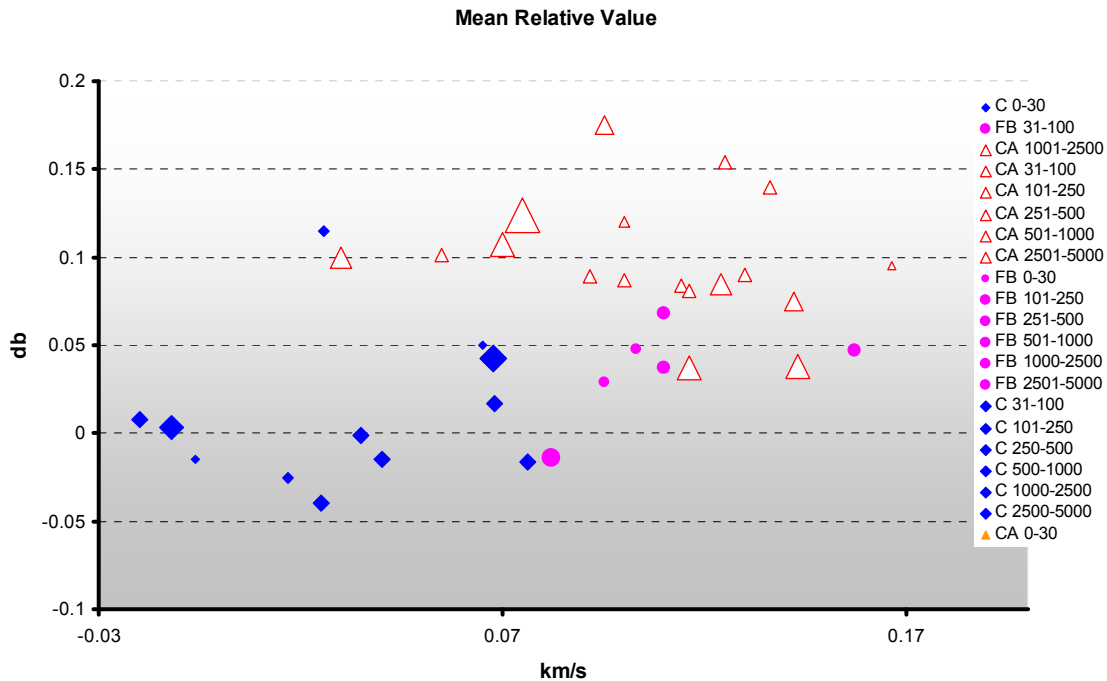


Figure 8: A plot of mean attenuation (vertical axis) and sound speed (horizontal axis) values of 36 breast masses. The biopsy results were used to determine the nature of each mass. The orange triangles represent cancer, the magenta circles are fibroadenomas and the blue diamonds are cysts. The size of each symbol is proportional to the original mass sizes.

Inspection of Figure 8 shows distinct groupings. The cancers occupy the upper right quadrant (high sound speed, high attenuation), the fibroadenomas populate the middle right portion while the cysts occupy the bottom left quadrant. These distributions are consistent with the original findings and suggestions by Greenleaf¹⁴. In ongoing work, we are adding more mass measurements to the data set and we are utilizing reflection parameters with the goal of further separating the above groupings and assessing the specificity of this technique. These results will be presented in a future paper.

4. CONCLUSIONS

Analysis of clinical breast images reconstructed from simultaneous acquisitions of reflection and transmission data are presented. These results indicate that operator-independent whole-breast imaging and the detection of cancerous breast masses are feasible using ultrasound tomography techniques. Our techniques successfully demonstrate tomographic imaging of breast anatomy. Furthermore, thresholding techniques allow us to obtain multi-parameter views of breast masses. A quantitative analysis of attenuation and sound speed values suggest a possible differentiation of cancer from benign masses, on the basis of these two parameters alone. Ongoing studies are aimed at (i) introducing reflection parameters to further improve the accuracy of mass differentiation and (ii) expanding the analysis to a 150 patient data set obtained with the latest version of the prototype. The results of these studies will be presented in a future paper.

5. REFERENCES

- [1] Berry DA, et al., Effect of Screening and Adjuvant Therapy on Mortality from Breast Cancer. N Engl J Med. 2005; 1784-1792
- [2] Gotzsche PC, Olsen O. Is screening for breast cancer with mammography justifiable? Lancet 2000; 355:129–134.
- [3] van den Biggelaar FJ, Nelemans PJ, Flobbe K. Performance of radiographers in mammogram interpretation: a systematic review. Breast. 2008; 17:85-90.
- [4] Schell MJ, Yankaskas BC, Ballard-Barbash R, Qaqish BF, Barlow WE, Rosenberg RD, Smith-Bindman R. Evidence-based target recall rates for screening mammography. Radiology. 2007; 243:681-9.
- [5] Armstrong K, Moye E, Williams S, Berlin JA, Reynolds EE. Screening mammography in women 40 to 49 years of age: a systematic review for the American College of Physicians. Ann Intern Med. 2007; 146:516-26
- [6] Turnbull, LW. Dynamic contrast-enhanced MRI in the diagnosis and management of breast cancer. J NMR Biomed 2008.
- [7] Jansen, SA, Fan, X, Karczmar, GS, Abe, H, Schmidt, RA, Newstead, GM. Differentiation between benign and malignant breast lesions detected by bilateral dynamic contrast-enhanced MRI: A sensitivity and specificity study. MAGNETIC RESONANCE IN MEDICINE. 59, 4, 747, 2008. John Wiley & Sons, Ltd
- [8] Kuhl CK, Schrading S, Bieling HB, Wardelmann E, Leutner CC, Koenig R, Kuhn W, Schild HH. MRI for diagnosis of pure ductal carcinoma in situ: a prospective observational study. Lancet. 2007; 370:485-92.
- [9] Saslow D, Boetes C, Burke W, Harms S, Leach MO, Lehman CD, Morris E, Pisano E, Schnall M, Sener S, Smith RA, Warner E, Yaffe M, Andrews KS, Russell CA; American Cancer Society Breast Cancer Advisory Group. American Cancer Society guidelines for breast screening with MRI as an adjunct to mammography. CA Cancer J Clin. 2007; 57:75-89.
- [10] Kolb, T.M., Lichy, J. and Newhouse, J.H. Comparison of the Performance of Screening Mammography, Physical Examination, and Breast US and Evaluation of Factors that Influence Them: An Analysis of 27,825 Patient Evaluation. Radiology. 2002; 225: 165 - 175
- [11] ACRIN website: www.acrin.org.
- [12] Wendie A. Berg, MD, PhD; Jeffrey D. Blume, PhD; Jean B. Cormack, PhD; Ellen B. Mendelson, MD; Daniel Lehrer, MD; Marcela Böhm-Vélez, MD; Etta D. Pisano, MD; Roberta A. Jong, MD; W. Phil Evans, MD; Marilyn J. Morton, DO; Mary C. Mahoney, MD; Linda Hovanessian Larsen, MD; Richard G. Barr, MD, PhD; Dione M. Farria, MD, MPH; Helga S. Marques, MS; Karan Boparai, RT; for the ACRIN 6666 Investigators. Combined Screening With Ultrasound and Mammography vs Mammography Alone in Women at Elevated Risk of Breast Cancer. JAMA. 2008;299(18):2151-2163
- [13] Zhou M, Johnson N, Blanchard D, Bryn S, Nelson J. Real-world application of breast-specific gamma imaging, initial experience at a community breast center and its potential impact on clinical care. Am J Surg 2008; 195:631-5.
- [14] J. F. Greenleaf, A. Johnson, R. C. Bahn, B. Rajagopalan: *Quantitative cross-sectional imaging of ultrasound parameters.* 1977 Ultrasonics Symposium Proc., IEEE Cat. # 77CH1264-1SU, pp. 989- 995, 1977.
- [15] Carson PL, Meyer CR, Scherzinger AL, Oughton TV. Breast imaging in coronal planes with simultaneous pulse echo and transmission ultrasound. Science. 1981 Dec 4;214(4525):1141-3.
- [16] M. P. Andre, H.S. Janee, P. J. Martin, G. P. Otto, B. A. Spivey, D. A. Palmer, "High-speed data acquisition in a diffraction tomography system employing large-scale toroidal arrays," International Journal of Imaging Systems and Technology 8, pp.137-147, 1997.
- [17] Johnson S. A., Borup, D. T., Wiskin J. W., Natterer F., Wuebbli F., Zhang Y., Olsen C. *Apparatus and Method for Imaging with Wavefields using Inverse Scattering Techniques.* United States Patent 6,005,916 (1999).
- [18] Marmarelis, V.Z., Kim, T., Shehada, R.E. Proceedings of the SPIE: Medical Imaging 2003; San Diego, California; Feb. 23-28, 2002. Ultrasonic Imaging and Signal Processing – Paper 5035-6.
- [19] Liu, D.-L., and Waag, R. C. "Propagation and backpropagation for ultrasonic wavefront design," IEEE Trans. on Ultras. Ferro. and Freq. Contr. 44(1):1-13 (1997).
- [20] Duric N, Littrup PJ, Babkin A, Chambers D, Azevedo S, Kalinin A, Pevzner R, Tokarev M, Holsapple E, Rama O, and Duncan R. Development of Ultrasound Tomography for Breast Imaging: Technical Assessment. Medical Physics. Vol. 32, No. 5, pp. 1375–1386, May 2005.
- [21] Duric N, Littrup PJ, Poulo L, et al. Detection of breast cancer with ultrasound tomography: First results with the Computed Ultrasound Risk Evaluation (UST) prototype. Med. Phys. 2007; 34: 773-785.